SCIENTIFIC REPORTS

OPEN

SUBJECT AREAS:
NONLINEAR OPTICS
TERAHERTZ OPTICS

Received
7 February 2014

Accepted
2 May 2014

Published
5 June 2014

Correspondence and requests for materials should be addressed to S.H. (shayashi@riken.jp)

Ultrabright continuously tunable terahertz-wave generation at room temperature

Shin'ichiro Hayashi[1], Kouji Nawata[1], Takunori Taira[2], Jun-ichi Shikata[3], Kodo Kawase[1,4] & Hiroaki Minamide[1]

[1]RIKEN, 519-1399 Aramakiaoba, Aoba, Sendai 980-0845, Japan, [2]Institute for Molecular Science, 38 Nishigo-Naka, Myodaiji, Okazaki 444-8585, Japan, [3]Nihon Univ., 1 Nakagawara, Tokusada, Tamura, Koriyama 963-8642, Japan, [4]Nagoya Univ., Furo-cho, Chikusa, Nagoya 464-8603, Japan.

The hottest frequency region in terms of research currently lies in the 'frequency gap' region between microwaves and infrared: terahertz waves. Although new methods for generating terahertz radiation have been developed, most sources cannot generate high-brightness terahertz beams. Here we demonstrate the generation of ultrabright terahertz waves (brightness ~0.2 GW/sr·cm^2, brightness temperature of ~10^{18} K, peak power of >50 kW) using parametric wavelength conversion in a nonlinear crystal; this is brighter than many specialized sources such as far-infrared free-electron lasers (~10^{16} K, ~2 kW). We revealed novel parametric wavelength conversion using stimulated Raman scattering in $LiNbO_3$ without stimulated Brillouin scattering using recently-developed microchip laser. Furthermore, nonlinear up-conversion techniques allow the intense terahertz waves to be visualized and their frequency determined. These results are very promising for extending applied research into the terahertz region, and we expect that this source will open up new research fields such as nonlinear optics in the terahertz region.

Exploiting nonlinear optical phenomenon in nonlinear materials allows a wide range of electromagnetic waves, from microwave to ultraviolet frequencies, to be produced and harnessed in a variety of applications. The terahertz region is relatively unexplored, because of the lack of the high-brightness terahertz sources, which has resulted in what is known as the frequency gap[1–3]. Over the past decade, there has been remarkable growth in the field of terahertz frequency science and engineering, which has become a vibrant, international, cross-disciplinary research activity[4]. Wavelength conversion in nonlinear optical materials is an effective method for generating and detecting coherent terahertz wave radiation owing to the high conversion efficiency, bandwidth, wide tunability, and room-temperature operation. Table 1 lists the characteristics of three intense terahertz-wave sources: our injection-seeded terahertz-wave parametric generator (is-TPG), and typical intense terahertz-wave sources; a far-infrared free-electron laser[5], and terahertz pulse generation by tilted pulse-front excitation[6]. Our source is one of the brightest in the terahertz region with a wide tuning range. We explain in this letter how the ultrabright terahertz waves are generated and visualized efficiently via acoustic phonons of a nonlinear lithium niobate ($LiNbO_3$) crystal.

The large figure of merit (FOM $\equiv 4d_{eff}^2 / n_{NIR}^2 n_{THz} \alpha_{THz}^2 \sim 10$, d_{eff} : the effective nonlinear coefficient, n_{NIR} and n_{THz} : the refraction indices in the near infrared and terahertz range, α_{THz} : the intensity absorption coefficient for the terahertz-wave)[6] of $LiNbO_3$ at room temperature makes this well-known nonlinear crystal ideal for such an application; terahertz wave parametric generation and detection in $LiNbO_3$ are realized by stimulated polariton scattering via transverse optical phonons[7–11]. However, a number of other nonlinear processes also occur when a high-intensity laser beam propagates through a nonlinear crystal; some examples include second-, third-, or higher-harmonic generation, sum or difference frequency generation, optical parametric amplification, oscillation, or generation, stimulated Raman or Brillouin scattering (SRS and SBS), four-wave mixing, optical rectification, multi-photon absorption, and the Kerr and Pockels effects. Of these, we found that SBS inhibits the parametric wavelength conversion near the lattice resonance induced by SRS, however, this nonlinear process has long been ignored. In principle, when a pumping photon generates an idler and a terahertz wave photon, the conversion efficiency reaches 10^{-3} according to the Manley–Rowe relations because the wavelength of the terahertz wave is about 200 times longer than that of the pumping beam. However, in previous research, the conversion efficiency from an infrared pumping beam to a terahertz wave was less than 10^{-7}. It has long been

Table 1 | Characteristics of intense terahertz-wave sources: our injection seeded terahertz-wave parametric generator (is-TPG), a free electron laser that works in the far-infrared region (FIR-FEL), and THz pulse generation through optical rectification using a tilted optical pulse front (OR). The brightness temperature (T_B) is calculated as $k_B T_B$ = Peak power/[$(M^2)^2$ × linewidth]. OR generates broadband terahertz waves

	Peak power [kW]	Linewidth [GHz]	T_B [K]	Tuning range [THz]
is-TPG	>50	~4	$\sim 10^{18}$	0.7–3
FIR-FEL	~2	~10	$\sim 10^{16}$	1–5
OR	~5000	~1500	$\sim 10^{17}$	

thought that this is the limit of the conversion efficiency using parametric wavelength conversion pumped by nano-seconds (duration: 10–25 ns) pulse lasers[10]. In our experiment, a pumping beam excites acoustic phonons in $LiNbO_3$ and SRS of the pumping beam generates terahertz waves and an idler beams. We calculated the SRS and SBS gains in previous condition, the SBS has 1000 times larger gain than the SRS[12–17]. Typically, the SBS gain reaches the steady state within ten lifetimes of the acoustic phonon[18], within about 1.5 ns in $LiNbO_3$[17]. For efficient frequency conversion, the duration of the pumping beam should be less than 1 ns, but the duration limits the linewidth of the generated terahertz waves. By exploiting a single-mode oscillated microchip Nd:YAG laser[19] with a sub-nanosecond 'pulse gap' pulse width[20], a narrow linewidth, high-efficiency wavelength conversion can be performed by the SRS without the SBS. If the intensity of the pumping source is too high, secondary (idler) beams can be generated, which do not contribute to the generation of terahertz waves as they undergo strong absorption. We thus precisely controlled both the pumping and seeding intensity as well as the crystal length.

In our experimental setup (Fig. 1), the pumping beam from the microchip Nd:YAG laser is amplified in two Nd:YAG rods in a double-pass configuration[21]. The seeding beam from an external cavity diode laser (ECDL) is amplified by an Yb-doped fiber amplifier. Owing to the grating and confocal arrangement, the noncollinear phase matching condition is satisfied automatically when the wavelength of the seeding beam is changed[22]. The terahertz-wave output extracted through the Si-prism was measured using a calibrated pyroelectric detector (THZ5I-MT-BNC; Gentec-EO) with two lenses (Tsurupica, Broadband Inc.), attenuators (TFA; CDP Corp.), an optical chopper, and a thick black polyethylene sheet for precise measurements. The temporal waveform and linewidth of the terahertz wave were measured by a Schottky barrier diode (SBD) and a pair of metal mesh plates. For the nonlinear up-conversion detection, the terahertz wave was focused onto another MgO:$LiNbO_3$ crystal. The incident angle between the terahertz wave and the pumping beam satisfies the noncollinear phase-matching conditions in the MgO:$LiNbO_3$ crystal. Mixing the terahertz wave with the pumping pulse created a narrow-linewidth difference-frequency up-converted signal, which was parametrically amplified by the MgO:$LiNbO_3$ optical parametric amplifier. The up-converted signals were visualized using an infrared laser visualizer (10VIZ-35; Standa Corp.) as green lights; the frequency was determined from the blinking position. All the components, except for the terahertz-wave detector, were mounted on a 60 × 90 cm^2 breadboard.

The brightness (peak power) as a function of the frequency (Fig. 2a) was obtained by scanning the wavelength using the ECDL as a tunable seeder. When the pumping energy was 20 mJ/pulse (duration: 420 ps, peak power: 48 MW) and the seeding power was 800 mW (continuous wave), the frequency could be tuned from 0.7–3 THz, and the maximum output brightness (peak power) was more than 0.2 GW/sr·cm^2 (50 kW) at around 1.8 THz. This source has a broad tuning range, with a flat region around 1.6–2.6 THz. The terahertz-wave output decreased in the low and high frequency

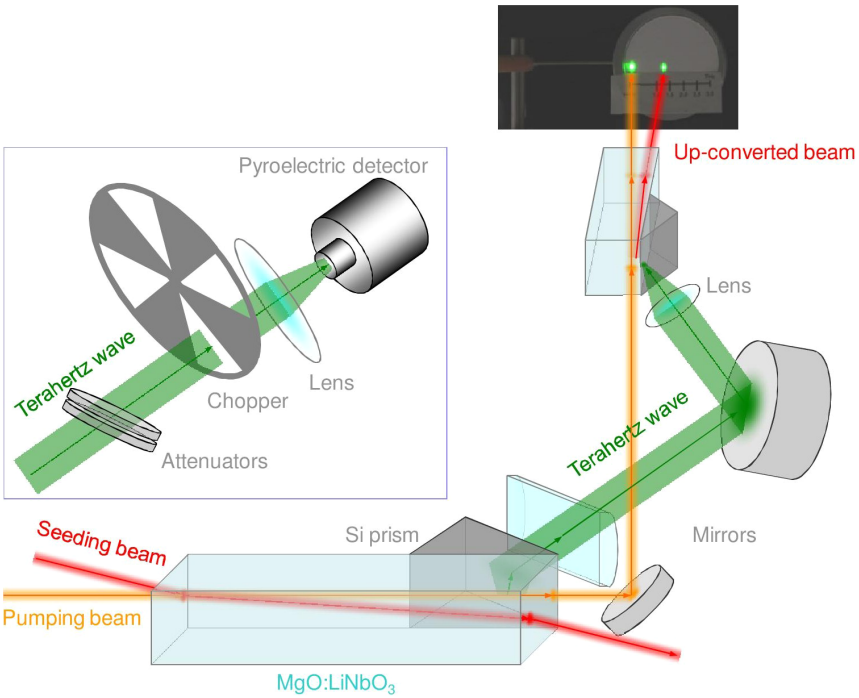

Figure 1 | Experimental setup. The diameter of the pumping beam on the nonlinear crystal is about 1.5 mm (full width at half maximum (FWHM)). The wavelength conversion is performed in a 50-mm-long nonlinear MgO-doped congruent $LiNbO_3$ (MgO:$LiNbO_3$) crystal with an antireflection coating for a wavelength of 1064 nm. A Si-prism placed on the surface of the MgO:$LiNbO_3$ crystal acts as an efficient output or input coupler for the terahertz wave to prevent total internal reflection of the terahertz wave at the crystal surface. Inset: the setup for the absolute power measurement using the calibrated pyroelectric detector (THZ5I-MT-BNC, Gentec-EO).

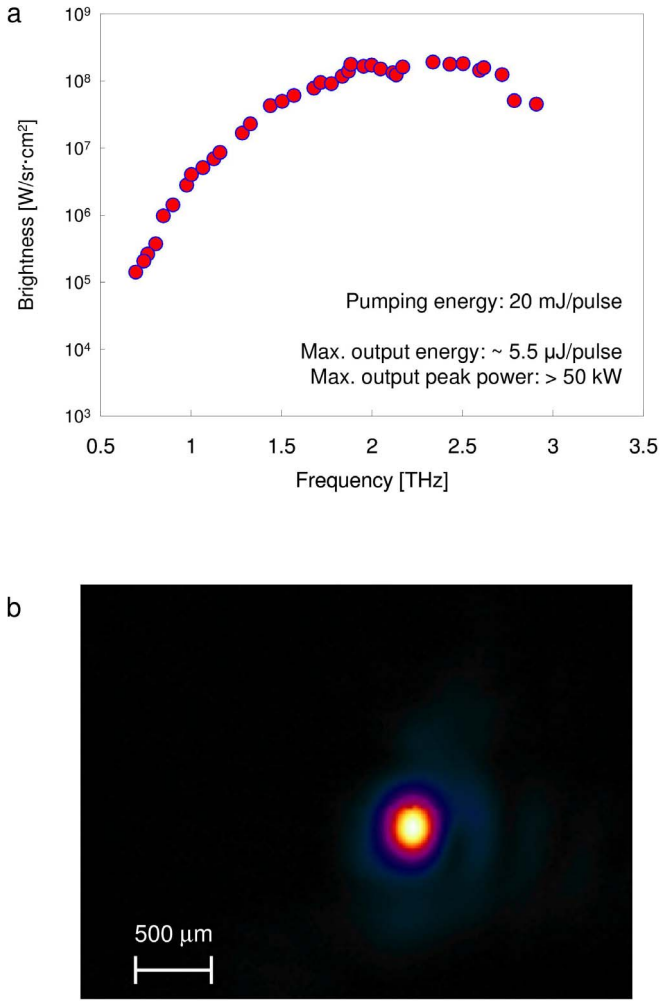

Figure 2 | Characteristics of our source. (a). The brightness as a function of frequency. (b). The beam profile of the terahertz wave measured by a terahertz-wave imager (IRV-T0831, NEC). The terahertz wave is focused by the f = 50 mm lens. The spot size is less than 220 μm (FWHM) at 1.5 THz.

regions (below 1.6 and above 2.6 THz) because of a low gain and high absorption coefficient[23] in these regions, respectively. From our source, the pulsed terahertz-waves are generated by 100 Hz (by 10 ms), however, this pyroelectric detector only gives an average power. We therefore used an optical chopper to measure the average power. We estimated the energy/pulse from the calibrated average power, the maximum energy was about 5.5 μJ/pulse. In this case, the output signal from this detector was more than 50 V_{PP}, corresponding to about 10^5 V_{PP} using a standard 4-K Si bolometer (Infrared Laboratories). When the glass plate was inserted, the output signal from the detector completely disappeared. We measured the duration of generated terahertz-wave around 100 ps by the SBD, corresponding peak power of more than 50 kW at 1.8 THz. Figure 2b shows a beam profile of generated terahertz-wave measured by an imager for terahertz-wave (IRV-T0831, NEC). The terahertz-wave is focused by the f = 50 mm Tsurupica lens. When the wavelength of input terahertz wave is 200 μm, the spot size is less than 220 μm (FWHM). We estimated the M^2 value less than 1.1, and the brightness was $B = Pp/(\lambda M^2)^2 \sim 0.2$ GW/sr·cm². The linewidth of the generated terahertz was measured to be almost 4 GHz by a scanning Fabry–Perot etalon. The intensity and electric field were 0.3 GW/cm² and ~0.5 MV/cm at around 2.0 THz, respectively, when the terahertz wave was focused. The high-power emission is also important for the calibration of terahertz wave detectors. In general, the power calibration is based on calorimetry as a traceable standard, but there is no power standard in the terahertz region. The power levels obtained from two kinds of pre-calibrated detectors, a calorimetric device (PM4, Erickson Inc.) and this pyroelectric device, using the same terahertz beam were comparable[24]. Surprisingly, this was easily perceived directly by touch; the wave was felt to be similar to a 100-Hz stimulation. The conversion efficiencies to the idler- and the terahertz- wave were more than 20% and 0.02%, respectively, which is improved by a factor of more than 1000 as a result of the nanosecond pumping source[10]. Under our experimental conditions, the observed conversion efficiency is 10^{-4} because the terahertz wave generated inside the crystal is absorbed by the nonlinear crystal itself while propagating to the crystal surface and is affected by Fresnel loss on the boundary surfaces[23].

Figure 3 shows the position of the up-converted signals as a function of the frequency of input terahertz wave. The red circles represent measured distance from the pumping beam, and the blue line represents the calculation results. Insets show the picture of the up-converted signals on the laser beam visualizer. The intensity and position of the up-converted signal depend on the power and frequency of the input terahertz wave respectively. As the power (frequency) of the input terahertz wave increases, the power and noncollinear phase-matching angle between the pumping beam and up-converted beam also increase, which shifts the position of the signal. This is in good agreement with the calculation, and this makes it easy to identify the frequency and intensity of the input terahertz wave from the position and intensity of the up-converted signal. When the energy of the input terahertz wave and pumping beam were 1 μJ/pulse at 1.9 THz and 10 mJ/pulse, respectively, the energy of the up-converted signal was 2 mJ/pulse at 1072 nm.

We have demonstrated here high-peak-power, narrow-linewidth, continuously tunable terahertz wave generation via wavelength conversion in MgO:$LiNbO_3$ having more than 10^5 times higher peak power than the peak power of terahertz-wave from our long pulse pumped (~15 ns) parametric sources by using half energy and 1/30 duration pumping pulse. We found this huge difference in peak power result from the suppression of the SBS in a nonlinear crystal by using sub-nanoseconds (420 ps) pumping pulse. Furthermore, the parametric gain (absorption) of the terahertz wave in $LiNbO_3$ could be increased (decreased) by cooling the crystal[25]. The conversion efficiency improves by a factor of at least ten at liquid nitrogen temperatures. In this case, for a pumping energy of 50 mJ/pulse, the expected brightness, brightness temperature, peak power and electric field of the terahertz wave are greater than 4 GW/sr·cm², 10^{19} K, 1 MW and 2 MV/cm, respectively from our narrowband and continuously tunable source. There are some other ways to generate much higher electric field at THz-GAP using different methods[6,26–28]. There results show higher electric field in this region, however, they generated broadband and a few cycles (pico-seconds duration) terahertz-wave. With the development of such intense broadband sources, nonlinear effects in this region have been observed[29–34]. On the other hand, a number of applications require intense, narrowband terahertz waves such as observing multi-photon absorption to specific excitation states[35,36]. The generation of narrowband megawatts peak power monochromatic terahertz-wave (sub-nanoseconds duration, several hundreds cycles) pulses with field levels in the megavolt per centimeter range will enable novel applications in terahertz nonlinear optics. We also demonstrated the visualization of generated terahertz waves using nonlinear up-conversion, which is similar to a wavelength dispersive spectrometer. Additionally, this method also provides phase information of the terahertz wave through the interaction with a simultaneously generated terahertz wave and the idler beam, and furthermore, works as a terahertz-wave amplifier by extracting the terahertz waves generated in a detection crystal. We speculate that the ultrabright terahertz-wave and its

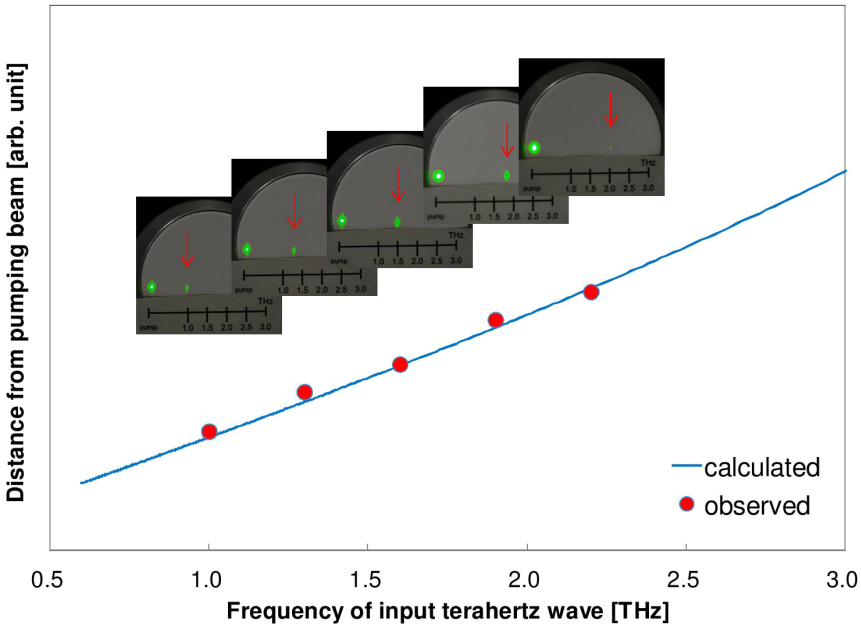

Figure 3 | The visualized up-conversion detection of the terahertz-wave. Measured position of the up-converted signals as a function of the frequency of input terahertz wave. The red circles represent the distance from the pumping beam when the frequency of the input terahertz waves are 1.0-, 1.3-, 1.6-, 1.9-, and 2.2-THz, and the blue line represents the calculation results from the noncollinear phase-matching angle, insets show the picture of the pumping and up-converted signal in each frequency. The left and right green spots represent the pumping beams and up-converted signals, respectively. As the frequency of the input terahertz wave is increased, the phase-matching angle between the pumping beam and the up-converted beam also increases such that the position of the up-converted signal moves depending on the noncollinear phase matching condition. We are then able to ascertain the frequency and intensity of the input terahertz wave from the position and intensity of the up-converted signal.

visualization could be powerful tools not only for solving real world problems but also fundamental physics, such as real-time spectroscopic imaging, remote sensing, 3D-fabrication, and manipulation or alteration of atoms, molecules, chemical materials, proteins, cells, chemical reactions, and biological processes. We expect that these methods will open up new fields and tune up killer applications.

1. Tonouchi, M. Cutting-edge terahertz technology. *Nat. Photonics* **1**, 97–105 (2007).
2. Chamberlain, J. M. Where optics meets electronics: recent progress in decreasing the terahertz gap. *Philos. Trans. R. Soc. London A* **362**, 199–213 (2004).
3. Sherwin, M. Terahertz power. *Nature* **420**, 131–132 (2002).
4. Linfield, E. Terahertz applications - A source of fresh hope. *Nat. Photonics* **1**, 257–258 (2007).
5. Rarnian, G. The new UCSB free-electron lasers. *Nucl. Instrum. Methods Phys. Res., Sect. A* **318**, 225–229 (1992).
6. Hebling, J., Yhe, K. L., Hoffmann, M. C., Bartal, B. & Nelson, K. A. Generation of high-power terahertz pulses by tilted-pulse-front excitation and their application possibilities. *J. Opt. Soc. Am. B* **25**, B6–B19 (2008).
7. Henry, C. H. & Garrett, C. G. B. Theory of parametric gain near a lattice resonance. *Phys. Rev.* **171**, 1058–1064 (1968).
8. Piestrup, M. A., Fleming, R. N. & Pantell, R. H. Continuously tunable submillimeter wave source. *Appl. Phys. Lett.* **26**, 418–421 (1975).
9. Kawase, K., Shikata, J., Imai, K. & Ito, H. Transform-limited, narrow-linewidth, terahertz-wave parametric generator. *Appl. Phys. Lett.* **78**, 2819–2821 (2001).
10. Kawase, K., Shikata, J. & Ito, H. Terahertz wave parametric source. *J. Phys. D: Appl. Phys.* **34**, R1–R14 (2001).
11. Guo, R., Ohno, S., Minamide, H., Ikari, T. & Ito, H. Highly sensitive coherent detection of terahertz waves at room temperature using a parametric process. *Appl. Phys. Lett.* **93**, 021106 (2008).
12. Agramal, G. P. Stimulated Brillouin Scattering. *Nonlinear Fiber Optics. Third ed.* Kelly, P. L., Kaminow, I. & Agrawal, G. P. (ed.) 355–362 (Academic Press, San Diego, 1995).
13. Weis, R. S. & Gaylord, K. Lithium Niobate: Summary of Physical Properties and Crystal Structure. *Appl. Phys. A* **37**, 191–203 (1985).
14. Dmitriev, V. G., Gurzadyan, G. G. & Nikogosyan, D. N. Properties of Nonlinear Optical Crystals. *Handbook of Nonlinear Optical Crystals. Third Revised Edition.* Schawlow, A. L., Tamir, T. & Siegman, A. E. (ed.) 119 (Springer, Berlin, 1990).
15. Hinkov, V., Barth, M. & Dransfeld, K. Acoustic Properties of Proton Exchanged $LiNbO_3$ Investigated by Brillouin Scattering. *Appl. Phys. A* **38**, 269–273 (1985).
16. Sussner, H. & Vacher, R. High-precision measurements of Brillouin scattering frequencies. *Appl. Opt.* **18**, 3815–3818 (1979).
17. de Bemabe, A., Prieto, C. & de Andres, A. Effect of stoichiometry on the dynamic mechanical properties of $LiNbO_3$. *J. Appl. Phys.* **79**, 143–148 (1996).
18. Faris, G. W., Jusinski, L. E. & Hickman, A. P. High-resolution stimulated Brillouin gain spectroscopy in glasses and crystals. *J. Opt. Soc. Am. B* **10**, 587–599 (1993).
19. Sakai, H., Kan, H. & Taira, T. >1 MW peak power single-mode high-brightness passively Q-switched Nd^{3+}:YAG microchip laser. *Opt. Express* **16**, 19891–19899 (2008).
20. Taira, T. Domain-controlled laser ceramics toward giant micro-photonics. *Opt. Mat. Express* **1**, 1040–1050 (2011).
21. Hayashi, S. *et al.* High-power, single-longitudinal-mode terahertz-wave generation pumped by a microchip Nd:YAG laser. *Opt. Express* **20**, 2881–2886 (2012).
22. Imai, K., Kawase, K., Minamide, H. & Ito, H. Achromatically injection-seeded terahertz-wave parametric generator. *Opt. Letters* **27**, 2173–2175 (2002).
23. Hayashi, S. *et al.* Output power enhancement of a palmtop terahertz-wave parametric generator. *Appl. Opt.* **46**, 117–123 (2007).
24. Dobroiu, A. & Otani, C. Calibration of terahertz-wave detectors: comparison procedure and error estimation. Proceedings of the 3rd EOS Topical Meeting on Terahertz Science & Technology, ISBN 978-3-9815022-1-3 (2012).
25. Shikata, J., Sato, M., Taniuchi, T., Ito, H. & Kawase, K. Enhancement of terahertz-wave output from $LiNbO_3$ optical parametric oscillator by cryogenic cooling. *Opt. Lett.* **24**, 202–204 (1999).
26. Hirori, H., Doi, A., Blanchard, F. & Tanaka, K. Single-cycle terahertz pulses with amplitudes exceeding 1 MV/cm generated by optical rectification in $LiNbO_3$. *Appl. Phys. Lett.* **98**, 091106 (2011).
27. Junginger, F. *et al.* Single-cycle multiterahertz transients with peak fields above 10 MV/cm. *Opt. Lett.* **35**, 2645–2647 (2010).
28. Clerici, M. *et al.* Wavelength Scaling of Terahertz Generation by Gas Ionization. *Phys. Rev. Lett.* **110**, 253901 (2013).
29. Hirori, H., Nagai, M. & Tanaka, K. Excitonic interactions with intense terahertz pulses in ZnSe/ZnMgSSe multiple quantum wells. *Phys. Rev. B* **81**, 081305-1–81305-4 (2010).
30. Merbold, H., Bitzer, A. & Feurer, T. Second harmonic generation based on strong field enhancement in nanostructured THz materials. *Opt. Express* **19**, 7262–7273 (2011)
31. Fan, K. *et al.* Nonlinear Terahertz Metamaterials via Field-Enhanced Carrier Dynamics in GaAs. *Phys. Rev. Letters* **110**, 217404-1–217404-5 (2013).
32. Liu, M. K. *et al.* Terahertz-field-induced insulator-to-metal transition in vanadium dioxide metamaterial. *Nature* **487**, 345–348 (2012).
33. Hirori, H. & Tanaka, K. Nonlinear optical phenomena induced by intense single-cycle terahertz pulses. *IEEE J. Sel. Top. Quantum Electron.* **19**, 8401110 (2013).

34. Zhang, C. *et al*. Terahertz nonlinear superconducting metamaterials. *Appl. Phys. Letters* **102**, 081121-1–081121-4 (2013).
35. Kulipanov, G. N. *et al*. Research Highlights from the Novosibirsk 400 W average power THz FEL. *Terahertz Science and Technology* **1**, 107–125 (2008).
36. Yokoyama, K., Matsuoka, L., Kasajima, T., Tsubouchi, M. & Yokoyama, A. Quantum Control of Molecular Vibration and Rotation toward the Isotope Separation. *Proc. of the 5th Asian Symp. on Intense Laser Sci. (ASILS-5)* 113–119 (2010).

Acknowledgments

The authors appreciate the fruitful discussions with Prof. H. Ito, Dr. C. Otani, and Dr. K. Midorikawa of RIKEN and Dr. Sakai of Hamamatsu Photonics K. K. The authors also thank Mr. Shoji of RIKEN and Mr. Takyu of Tohoku University. This work was partly supported by Collaborative Research Based on Industrial Demand of the Japan Science and Technology Agency (JST) and Japan Society of the Promotion of Science (JSPS).

Author contributions

Experiments on terahertz-wave generation were done by S.H. and K.N. The theoretical analysis and estimation of SRS and SBS was performed by J.S. The pumping laser was developed by T.T. The main manuscript text and the all figures were written by S.H. K.K. and H.M. conceived and supervised the project. All authors have discussed and reviewed the manuscript.

Additional information

Supplementary information accompanies this paper at http://www.nature.com/scientificreports

Competing financial interests: The authors declare no competing financial interests.

How to cite this article: Hayashi, S. *et al*. Ultrabright continuously tunable terahertz-wave generation at room temperature. *Sci. Rep*. **4**, 5045; DOI:10.1038/srep05045 (2014).